



IMAGE BASED SURFACE TEMPERATURE EXTRACTION AND TREND DETECTION IN AN URBAN AREA OF WEST BENGAL, INDIA

Sk Ziaul*, Swades Pal

Department of Geography, University of Gour Banga, Malda 732103, West Bengal, India

* Corresponding author, e-mail: skziaul87@gmail.com

Research article, received 2 June 2016, accepted 25 October 2016

Abstract

Rapid urbanization and change of landuse/landcover results in changes of the thermal spectrum of a city even in small cities like English Bazaar Municipality (EBM) of Malda district. Monitoring the spatio-temporal surface temperature patterns is important, therefore, the present paper attempts to extract spatio-temporal surface temperature from thermal band of Landsat imageries and tries to validate it with factor based Land Surface Temperature (LST) models constructed based on six proxy temperature variables for selected time periods (1991, 2010 and 2014). Seasonal variation of temperature is also analyzed from the LST models over different time phases. Landsat TIRS based LST shows that in winter season, the minimum and maximum LST have raised up 2.32°C and 3.09°C in last 25 years. In pre monsoon season, the increase is much higher (2.80°C and 6.74°C) than in the winter period during the same time frame. In post monsoon season, exceptional situation happened due to high moisture availability caused by previous monsoon rainfall spell. Trend analysis revealed that the LST has been rising over time. Expansion and intensification of built up land as well as changing thermal properties of the urban heartland and rimland strongly control LST. Factor based surface temperature models have been prepared for the same period of times as done in case of LST modeling. In all seasons and selected time phases, correlation coefficient values between the extracted spatial LST model and factor based surface temperature model varies from 0.575 to 0.713 and these values are significant at 99% confidence level. So, thinking over ecological growth of urban is highly required for making the environment ambient for living.

Keywords: Land Surface Temperature, Landsat TIRS, factor based LST models

INTRODUCTION

Knowledge of Land Surface Temperature (LST) and its temporal and spatial variations within a city environment is of prime importance to the study of urban climate and human–environment interactions (Stathopoulou and Cartalis, 2009; Sharma and Joshi, 2013; Singh and Grover, 2014; Alavipanah et al., 2015). The retrieval of the LST from remotely sensed TIR data has attracted much attention, and its history dates back to the 1970s (McMillin, 1975). Urban heat island (UHI) and magnitude of the difference in observed ambient air temperature between cities and their surrounding rural regions have been a concern for more than 60 years (Landsberg, 1981). Nichol and Hang (2012) reported that there is a clear cut difference of temperature between rural and urban region and this gap is usually 3–4°C. One of the earliest UHI studies was conducted in 1964 (Nieuwolt, 1966) in the urban southern Singapore. Extensive urbanized surfaces modify the energy and water balance processes and influence the dynamics of air movement (Nichol and Hang, 2012). Afterward, many scientists (Giridharan et al., 2004; Neteler, 2010; Schwarz et al., 2011; Xiong et al., 2012; Zhang et al. 2013; Li et al. 2014; Kuang et al., 2015b; Alavipanah et al., 2015) have worked in this field emphasizing different cognitive issues.

LST is a key factor in physical dispensation of land surface at different spatial scale, and it generalizes the results of the interaction between land surface and atmosphere, exchange of matter and energy (Wan and Dozier, 1996; Alavipanah et al, 2015). In the general assessment model of sustainable development and LST change, the change of LST is regarded as an important criterion upon which the evaluation of environmental quality and social and economic development policy can be based (Keller, 2008; Dai et al., 2010). Dynamic variability of LST seasonally and diurnally encouraged scholars to address this fact. Seasonal variation is well documented by Yuan and Bauer (2007) and Deosthali (2000) and they found that at night, the center of the city appeared as both heat and moisture island whereas at the time of sunrise as heat and dry island.

In 2008 more than half of the world's population were urban dwellers and the urban population is expected to reach 81% by 2030 (UNFPA, 2007). This acceleration of urbanization is very high both in intensity and area in developing countries like India. So, studying of the environmental conditions is necessary for proper planning or policy review. At the same time, it is already established that low population density is associated with lower LST values (Li et al., 2014) and conversely it is true that higher temperatures are associated with densely populated urban areas.

Intensity of LST is related to patterns of land use/cover changes (LULC), e.g. the composition of vegetation, water and built-up and their changes (Ding and Shi, 2013; Li et al. 2014; Grover and Singh, 2015; Kuang et al, 2015 a, b). Both horizontal and vertical urban expansion, spacing between buildings, building materials, location of public places, bus stoppage, railway station, major and minor industrial hubs etc. influence temperature concentration (Park, 1986; Alavi-panah et al., 2015). Rising population and building density are also accelerating factors of LST (Schwarz et al., 2011; Peng et al., 2012). The spatial extent of concrete cover and material composition is another major vector of spatial pattern of LST (Xiong et al., 2012; Kuang et al., 2015b). Growing population density, greater consumption of energy etc. can also aggravate temperature condition (Zhang et al, 2013; Li et al., 2014).

Clearly, the built-up land exhibited the highest LST, followed by bare soil, water body, and vegetation in all three periods as reported by Weng (2001), Weng and Yang (2004) and Chen et al. (2006). In forested area, temperature is almost 4.5-5°C lower than bare land (Buyantuyev and Wu, 2010).

It has been shown from both a theoretical and a practical point of view that the Normalized Difference Vegetation Index (NDVI) derived from satellite data is a good indicator of vegetation density (Grover and Singh, 2015; Gulácsi and Kovács, 2015). Vegetation can reduce LST by 13°C and considered one of the dominant factors for better health condition and a positive human comfort (Gémes et al., 2016). Both directionality of values (positive and negative) carry important role for regulating surface temperature. Positive and negative respectively indicate high vegetation density and high moisture which can help to reduce surface temperature (Choudhury, 1987; Kibert, 2012). In most cases, a negative correlation between NDVI and LST is found (Xiao et al., 2007; Zhang et al., 2013), although high canopy cover area is not a prime determinant because plant species, leaf area, soil background, and shadow can all contribute to the NDVI variability (James and Charles, 2014). Yuan and Bauer (2007), Li et al. (2012) revealed that the relationship between NDVI and LST varies seasonally. James and Charles (2014) also established that water bodies exhibits minimum land surface temperature than other landuse/land cover.

Normalized Difference Building Index (NDBI) indicates built up area concentration over space. Most of the previous studies recorded high surface temperature in the urban built up areas (Chen et al., 2006; Liu and Zhang, 2011; Essa et al., 2012) although its magnitude varies significantly due to variability in composition of building materials and density of buildings. Vertical growth is also responsible for intensifying LST (Park, 1986). Yuan and Bauer (2007) suggested that the percentage impervious surface cover as a more reliable metric for quantitative analysis of LST over different seasons for urbanized areas. Major road axes and railway station are characterized by high traffic and population concentrations and often have a higher temperature (Weng et al., 2004).

For preparing multi criteria approach based spatial modeling in different sector, the use of GIS has received valued reputation (Carver, 1991; Eastman, 1997). The Boolean overlay operations (no compensatory combination rules) and

the weighted linear combination (WLC) methods (compensatory combination rules) are two major dimensions of multicriteria suitability modeling. They have been the most often used approaches for different sorts of landuse suitability analysis (Malczewski, 2004). All the previous work in this approach is based on weighted additive average of the data layers selected for the suitability models. But the way of providing weight to the data layers according to their importance are different. For weighting the data layers PCA based approach (Khatun and Pal, 2016), analytic hierarchical approach (AHP) (Satty, 1980) etc. are used.

Ground measurement cannot provide wide spread data of different places at a time therefore contribution of satellite-based thermal infrared data is applied frequently in the developed nations. In India, this advanced method for spatial surface temperature extraction is not often applied. Growing urbanization rate, intra-urban density etc. require such study for rethinking about renewal of urban planning based on satellite data based temperature analysis at different spatio-temporal scale. In the Third World Countries like India, the density of meteorological stations is so sparse over space (average density of meteorological station is 1/500 km², in plain region it is 1/520 km², in elevated land it is 1/260-390 km² and in hilly region it is 1/130 km² (Raghunathan, 2010) that there is no other alternative than to use TIR satellite data based temperature extraction. Another major advantage of this data is that it provides pixel to pixel temperature information and produces micro level variation of temperature over space. Such data also helps to predict the local driving factors of surface temperature. Kawashima et al. (2000) documented a relation between mean air temperature and mean surface temperature. Also they rightly mentioned that this relation varies with altitude. They recorded that mean air temperature is 7° to 9.6°C larger than the mean surface temperature and obviously difference is higher at lower elevation. Adjusted R² ranges from 0.91 to 0.98 when regression is carried out between spatial air temperature and LST distribution models because of their high spatial association.

Present paper attempts to capture spatio-temporal variation of land surface temperature over the English Bazar Municipality (EBM) and its peripheral areas of West Bengal state of India. Furthermore, a factor based LST model was developed for understanding the relative variation of temperature over the region. Comparison of the actual land surface temperature data extracted from TIR is done in response to the factor based LST models constructed using major controlling factors. Main motive behind the factor based modeling is to find out it can substitute TIR satellite data based LST model. Also it aims to investigate whether the selected factors are effective for explaining spatial LST patterns. Priority analysis of the local level driving factors of temperature variation is carried out to understand the dominant driving factor of LST. Seasonal variation of temperatures at each time period (pre-monsoon, monsoon and winter) is analyzed to show seasonal extremities in this sub humid urban region. Trend analysis of temperature in different seasons over the temporal scale is also carried for identifying changing degree and intensity of LST. In brief, two sets of LST models have applied in this work. First approach is Landsat TIR based LST modeling and second approach is proxy factor based LST

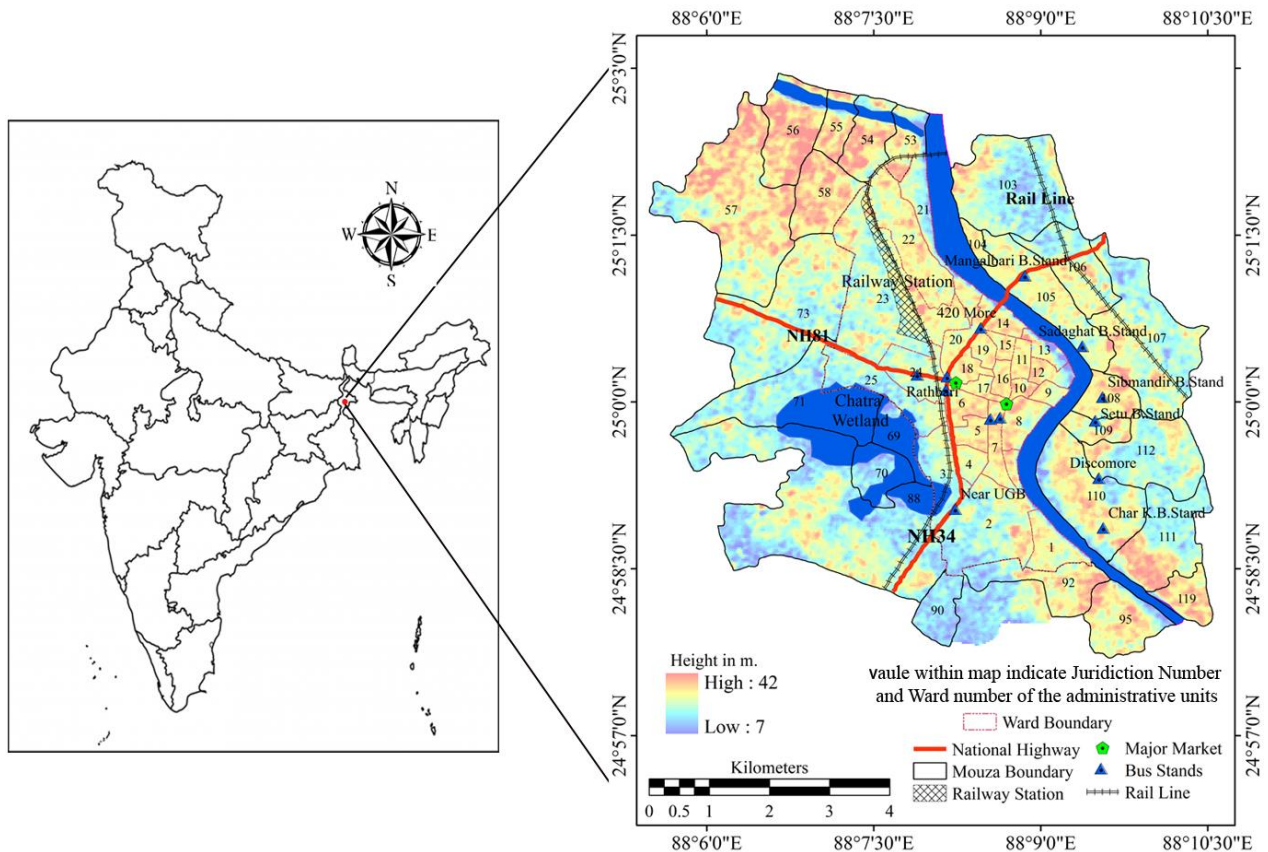


Fig. 1 Study sites showing selected mouzas, rivers, wetland, NH34, railway line, station and major market points

modeling for the same phases. Ultimately, spatial correlation coefficient between two sets of models have been calculated to test the accuracy of the factor based models.

STUDY AREA

The present study area consists of 29 wards of English Bazar Municipality (EBM), 16 surrounding mouzas (smallest administrative or land revenue unit) from English Bazar block and 11 mouzas from Old Malda block (relatively larger administrative unit composed with several mouzas) covering an area of about 5500 ha (Fig. 1). The entire study area comes under Diara tract of West Bengal with fertile fine grain silty clay carried out by river Ganga and its distributary Kalindri River and Mahananda River, located at the northern and eastern margins of the study area. The average elevation of the region is 17m above MSL.

The water table is moderately deep (5 m to 10 m under surface) with moderately high seasonal fluctuation (2-4m). (Central Ground Water Board, 2010) and it may control evaporation as well as land surface temperature.

North western part of the present study area is covered with mango orchards. Chattra wetland (perennial) is considered the lungs of the town, and is located at the boundary zone of the town. Over time, this wetland area is captured by built up area. Climate of this region is characterized by sub tropical monsoon with seasonal wet and dry spell of rainfall, cold and hot spell of temperature. The year is sub divided by four major seasons: (1) winter season (January and February), (2) pre-monsoon season (March to May) with little rain and high temperature and evaporation, (3) monsoon season (June to mid-October) with maximum (about 82% of total rain) rain and high temperature and (4) post-monsoon season (mid-October to mid-December) with steady decline of rainfall and temperature. The post monsoon effect is less distinct. Average annual rainfall of this basin as gauged by Malda meteorological station is 1444 mm. Monthly variation of rainfall and temperature is noticeable (Table 1). The average potential evaporation, being one of the controlling factors of surface temperature, was 73 mm/year between 1901 and 2014 in the area.

Table 1 Average monthly temperature and rainfall conditions between 1991 and 2014

Climatic indicator	January	February	March	April	May	June	July	August	Sept.	Oct.	Nov.	Dec.
Tmax (°C)	23	26.7	32.3	35	34.7	33.7	32.2	32.2	31.7	30.8	28.5	24.8
Tmin (°C)	10.1	12.1	16.5	21.7	24.3	25.7	25.9	26	25	22	16.9	11.9
Rainfall (mm)	10.9	10.8	11	39.1	117.5	229.4	353.1	302.4	296.6	91.8	12.3	10.3

The town possesses a good infrastructure and facilities. Two railway stations e.g. GourMalda and Malda town are located at southern and northern part of this area. Railway line and National High way (NH) 34 perforate the town from south to north. Two main markets, Netaji market/Rathbari market and Chittaranjan market are located at the heart of the town and are considered as Central business district (CBD) of this commercially improved town (see Fig. 1).

The total number of population and house hold in the study area are 291612 people and 61803 households respectively according to the census of 2011. Additionally, it is also needed to mention that apart from these, the amount of people in the city is more than 50 % higher due to people from outside the city. The town is the main market town of the larger catchment of the Malda, Murshidabad and Dinajpur districts of West Bengal and Larger part of Eastern Jharkhand state of India. Most of the cases, spacing between houses is about to 45-60cm, exemplifying the dense building pattern.

MATERIALS AND METHODS

Data and image pre-processing

Landsat 5 and Landsat 8 are used for both landuse/land-cover mapping and LST modeling (path/row 139/43; spatial resolution for TIR band of Landsat 5 is 120m and for

Landsat 8 it is 100m.; spatial resolution for other bands is 30m in Landsat 5 and band 1 to 7 for Landsat 8). The extraction of LST is based on Landsat satellite images acquired through the USGS Earth Resource Observation Systems Data Center, which are corrected for radiometric and geometrical distortions of the images to an acceptable quality level before delivery. The Landsat image is further rectified to a common Universal Transverse Mercator coordinate system. Noise diminution is essential for the thermal sensed satellite images, particularly for the thermal infrared (TIR) band. The inherent noise may affect the retrieval of brightness temperature or LST.

Methods

The methodology consists of three sections (Fig 2): extraction of LST from Landsat images, multicriteria LST modelling, spatial association between Landsat based LST model with multicriteria LST (McLST) model. The first section adopted two approaches for LST modeling. 1) Landsat TIR based extraction of LST and 2) Proxy temperature factor based multicriteria LST modeling. First approach is entirely based on thermal band of landsat images of different time periods and the second approach is based on six proxy temperature factors as indicated in Table 2. Entire methodological work flow is illustrated in Figure 2.

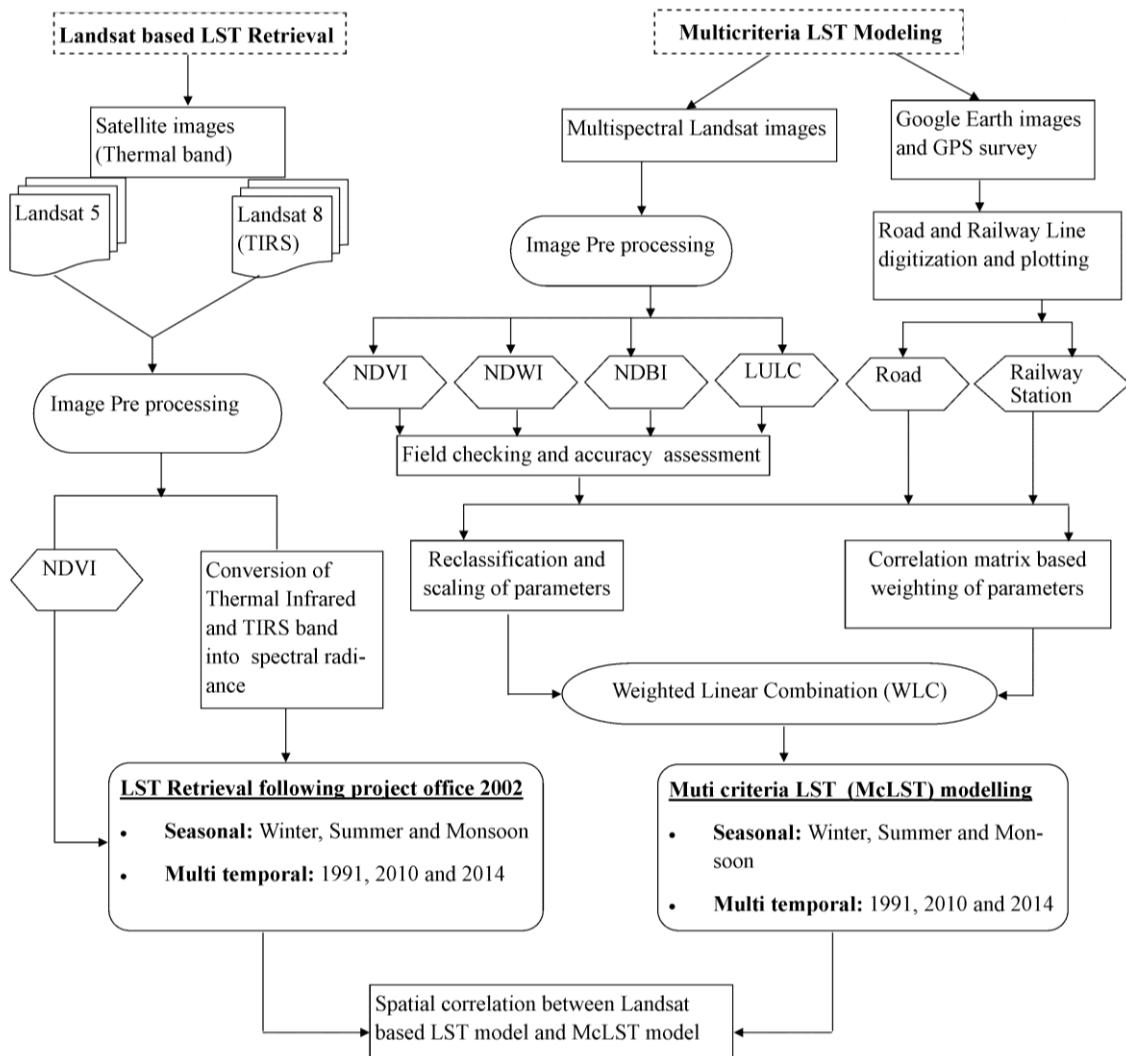


Fig. 2 Flow chart showing methodological workflow

Table 2 Selected proxy parameters and associated sources of data set

Name of the parameters	Source(s)
1) Land use	Sensor: Imageries of Landsat 5, Nov., 2013 (Path/Row:139/43; Band used: G, R, NIR; Spatial resolution: 30m.), Land use map, 2014 of Land reform Deptt., West Bengal
2) NDBI	Extracted from Landsat 5 and 8 images
3) NDVI	Satellite image of Landsat 5 and 8 based on Townshend and Justice, 1986
4) NDWI	Satellite image of Landsat 5 and 8 based on McFeeters, 1996
5) Major Road	Extracted from Google image, DST map, Malda district
6) Railway Station	Extracted from Google image and field check through GPS
7) Land surface temperature	TIRS 1 & TIRS 2 band of Landsat 8 and Thermal Infrared band of Landsat 5

LST extraction and modeling

Approach 1 deals with extraction of LST from thermal band of the selected sensors is well discussed with a good number of merits and demerits by the Xiong et al. (2012), Zhang et al, (2013), Li et. al. (2014). It is multistep methods i.e. Conversion of the Digital Number (DN) to Spectral Radiance, conversion of spectral radiance to at satellite brightness temperature, LST extraction, conversion of LST from Kelvin to degree Celsius. This method is quite different for each sensor (Landsat 5, 7 etc.). All these things are well defined in the respective guidelines published by Landsat Project Science Office (2002). In this present work, guidelines of the same have been followed for working out LST from Landsat imageries.

Approach 2 deals with six proxy data layers (Table 3). These layers are (1) Landuse/landcover, (2) Normalized differential Vegetation Index (NDVI) map, (3) Normalized differential water index (NDWI) map, (4) Normalized differential built up index (NDBI), (5) Major roads and (6) railway station. Here some other factors theoretically can be adopted like relief, rainfall etc. But these layers are not taken here because of their minimal influence within such a small spatial area.

As WLC process executes on the basis of raster based weighted linear combination (WLC), it is required to convert each with an equal. NDWI, NDVI, NDBI, landuse/landcover layers have been extracted as raster layers, so there is no need for conversion for these four layers. But other two layers i.e. major roads and railway station layers are in vector forms and these are needed to be converted into raster layers. For this, proximity maps have been constructed from these layers. It is assumed that the area nearer to the roads or railway lines or stations will be affected more by increased LST and gradually it will decrease with increasing distance from roads or railway lines. After converting the selected layers to raster format, each attribute (map layer) is categorized into 10 classes ranking 1 to 10, where a higher rank reflects a potentiality higher LST. Landuse/landcover classes have been ranked

based on the potential contribution toward LST. For example, built up class has assigned maximum weight. Here relative ranking of the landuse/landcover class is done based on subjective priority. To fulfill this purpose, all the attributes have been reclassified into 10 classes following natural break method and ranked accordingly. The logic behind ranking to intra attribute classes from 1-10 is described in Table 3. Weightage of each attribute has been defined objectively (Table 4) considering the degree of correlation of each driving factor with land surface temperature generated for different years. The logic behind this consideration is that highly correlated parameters maximally explain the spatial variation of temperature. Normalization of respective weights (values of r for respective parameters) based on dimension index have been performed for frame it in a scientific scale. It is calculated for distributing relative weight of all the parameters. Here total normalized weight is 1. The parameter shares maximum out of 1 is emerged as dominant parameter. The result of each normalized value is called attribute weight. Weights of the parameters for different seasons in respective years are different due to having some dynamic variables like landuse/landcover, built up area, water bodies, canopy coverage etc. Therefore nine models have been articulated for different seasons in the selected years.

Table 3 Modes of ranking of the intra sub class of parameters

Name of the attribute (j)	Highest rank indicates at 10 point scale	Logic behind
1) Land use	10 rank at built up land	Concrete area has high temperature emissivity
2) NDBI	10 rank at highest intensity class	High intensity built up land emits maximum temperature
3) NDVI	10 rank at '0' value	Above and below 0 value canopy cover and water availability increases which may reduce temperature
4) NDWI	10 rank at lowest NDWI value	It does indicate water concentration; more concentration of water bodies mean less temperature and vice versa
5) Major Road	10 rank at road adjacent zone	Highly dense traffic in all roads concerned specifically National High Way 34 insists temperature rise
6) Railway Station	10 rank at near to the railway station	Being a nodal centre, a good number of trains ups and down and huge number of passengers uses this station as nodal point

Expression of weight calculation is as follows (Eq. 1):

$$w_j = \frac{a_{j_r}}{\sum_{j=1}^n j_r} \quad (\text{Eq. 1})$$

where w_j =weight of j th parameter; a_{j_r} = correlation coefficient of j th attribute; \sum_{j_r} = summation of correlation of all j th variable.

Rank of all sub classes under each attribute is then multiplied by the defined weight of each individual attribute. This function can be presented using Equation 2:

$$WLC = \sum_{j=1}^n a_{ij} w_j \quad (\text{Eq. 2})$$

where, a_{ij} = ith rank of jth attribute; w_j = weightage of jth attribute. This weighted linear combination has been done using raster calculator tool in ArcGIS environment.

Weight of the attributes for different other periods has been calculated based on their respective correlation coefficient values. See table 6 for calculated weights of the parameters for different time phases. Calculation of the entire process is represented in Table 4 showing the case of January, 2014.

Table 4 Pattern of reclassification of the parameters, ranking and weighting of the parameters of January, 2014

Parameters	Sub-class	Rank	Weight of parameters
1) NDBI	natural breaks	1-10	0.382
2) NDVI	natural breaks	1-10	0.042
3) NDWI	natural breaks	1-10	0.064
4) Land use/ Land cover	Water Bodies & Water Hyacinth	1	0.336
	Mango Orchard	3	
	Agricultural Land	6	
	Fallow Land	8	
	Built up Land	10	
5) Major Road (Distance from major road)	natural breaks	1-10	0.154
6) Railway Station (Distance from station)	natural breaks	1-10	0.022

After preparing the multicriteria spatial LST model based on controlling factors and the Landsat TIR based LST model(s), spatial correlation coefficient between them has been calculated to judge the level of spatial association. Strong correlation coefficient (r) does mean higher level of spatial coincidence and vice-versa. Chen et al (2006) and Ogashwara and Brum Bastos (2012) focused on the quantitative relationship between LST and temperature controlling factors by using correlation coefficient analysis. In this present work, their line of thinking has been followed.

Methods for framing data layers used for multicriteria LST modeling

This section describes how NDVI, NDWI, NDBI and others have been prepared for constructing multicriteria LST models. For NDVI extraction, method of Townshend and Justice, (1986) is used.

$$NDVI = \frac{(NIR\ band - R\ band)}{(NIR\ band + R\ band)} \quad (\text{Eq. 3})$$

where, NIR=near infrared band (band 4 of MSS and TM), R=red band (MSS band 2, TM band 3). Values ranges from -1 to +1, where negative values normally are associated with water and where positive values indicate vegetation mass. In principle, higher values are linked with higher vegetation density.

For extracting NDWI, equation presented by McFeeters (1996) is used:

$$NDWI = \frac{(Green\ band - NIR\ band)}{(Green\ band + NIR\ band)} \quad (\text{Eq. 4})$$

where Green is the green band (MSS band 1, TM band 2) and NIR is the near infrared band (band 4 of MSS and TM). This value ranges from -1 to 1. Value nearer to 1 indicate greater possibility of low LST.

Normalized differential built up index (NDBI) has been calculated following Zha et al (2003):

$$NDBI = \frac{(MIR\ band - NIR\ band)}{(MIR\ band + NIR\ band)} \quad (\text{Eq. 5})$$

where, MIR is the mid infrared band (TM band 5, OLI band 6) and NIR is the near infrared band (TM band 4, OLI band 5). NDBI value ranges from -1 to 1. Value nearer to 1 means greater possibility of high LST.

The land use data set has been prepared from Landsat imageries of the respective periods mentioned in Table 2. Supervised image classification techniques (non-parametric rule: maximum likelihood) have been used for landuse/land-cover (LULC) classification. Accuracy assessment has been done by cross checking 139 sites through GPS survey and Google Earth images. From this assessment, it was found that the accuracy assessment generated from the supervised classification technique showed an overall classification accuracy of 84.45% with Kappa statistic of 0.829, which indicates a very good agreement (Monserud and Leemans, 1992) between thematic maps generated from image and the reference data.

Road and railway lines have been digitized from Google Earth image, toposheet of Survey of India and those vector layers have been converted into raster layers through proximity or distance mapping. Actually, ten equidistance buffer classes have been made both from roads and railway line individually.

Method for spatial association between Landsat based LST model with multicriteria LST (McLST) model

Most of the previous work across India in this field have extracted surface temperatures but these were not validated with any reference standard datasets collected from meteorological monitoring stations. As only one meteorological station is available over the present study area, it is difficult to validate the spatio-temporal data with meteorological data available there on. Authors here attempted to compare their models with some Multicriteria LST models created based on major locally dominant temperature driving factors. After extracting LST from TIRS of Landsat and constructing multicriteria LST model, simple

correlation coefficient (r) between these two layers for different seasons in the selected years has been calculated. It is being considered that higher degree of r value means strong spatial association. Student's 't' test has been carried out for assessing degree of significance level of the calculated correlation at 95% and 99% confidence levels. A strong spatial relation would indicate that multicriteria LST models can be used for assessing relative LST pattern over the study area.

For finding out dominant factor of LST, correlation coefficient of the selected factors with surface temperature layers of the respective periods have been calculated. Strongly correlated parameters are considered as dominant factors. This is calculated during Multicriteria LST model building.

RESULTS AND DISCUSSION

Results extracted from data layers

Earlier it is mentioned that six data layers have been prepared for constructing multicriteria LST modeling. In this section result of the individual layers has been depicted. Through supervised image classification, six number of major landuse/landcover classes have been identified with an accuracy level of 84.45% with Kappa statistic of 0.829. Out of total area (~5500 ha), 42.24% is covered with built up land followed by mango orchard (24.15%). The core part of the study area is composed of built up land and it spreads along the major roads and railway line outside the core. If only core area is considered, more than 78% of the area is built up area. Such built up area concentration is highly effective for enhancing LST. The NDBI pattern shows that the maximum intensities (NDBI score: 0.160-0.179) of built up area are found at the core part and also it increases even in the peripheral land. Over time, greater proportion of study area comes under this intensity of NDBI. NDVI value is recorded maximum (0.292-0.487) in the north western part of the study area where one denser mango orchard is located. Such value is only found in the peripheral part of the study area. This value decreases over time over the major parts, especially in the core parts. From this result it can be stated that there is a negative relation between NDBI and NDVI. NDWI values with maximum intensity are only (0.288-0.422) found in the river Mahananda at the eastern side and Chatra wetland at the western side of the study area.

Landsat image based LST change

Seasonal temperature dynamics (winter, pre-monsoon and monsoon) in 1991

Usually, temperature is confined within the range of 14.41-20.34°C during January, 1991 (Fig. 3A). Out of total area, 32.83% area represents temperature from 16.18 - 16.77°C followed by 24.8% area is represented by 16.77 - 17.37°C temperature. More than 83% is characterized by the temperature ranges from 16.18-18.55°C. Mean temperature of this study area in this time was 17.24°C and the coefficient of variation (CV) was 4.04%. Core urban area is sensitive to high temperature.

April and May of this year show that the maximum air temperature was 40°C or more. But at present case surface temperature ranges from 23.99°C to 34.64°C (Fig. 3B). Low antecedent moisture and lack of rainfall triggered by nor wester (a kind of local storm with rain) might enhanced temperature a little bit. Within this temperature spectrum, 29.31 - 30.37°C temperature covers 20.97% of the total area followed by 30.37 - 31.44°C temperature in 20.66% of the area. More than 81% area possesses temperature between 27.18-32.5°C. North western and south eastern part of the study area exhibit relatively low range of temperature due to the Bagbari mango orchard and Chatra wetland. Only in April, the wetland area is prominent due to its distinct oceanicity factor. Expectedly, areal coverage of high temperature is maximum in this time. From temperature condition, it is also clear that urban spread is maximum in the eastern part of the main town following river Mahananda and north western part of the main town along main concrete road (National Highway) which connects the western and north western part of the Malda district with district town (English Bazar Municipality).

In October of the monsoon month, due to frequent rainfall, despite having high temperature potential, temperature is self regulated. In this year temperature ranges from 21.66°C to 28.09°C (Fig. 3C). About 89% spatial extent is characterized by 22.30°C to 24.87°C temperatures. Spatial character of moisture availability regulates temperature over space. In temperature distribution, there is no such continuity as exhibited in figure 3C. Except main town most part of the peripheral area shows quite lower temperatures. Within main town variation of temperature is 27.64% and it is about 64.25% in the peripheral area.

Seasonal temperature dynamics (winter, pre-monsoon and monsoon) in 2010

In winter season, 2010 range of temperature was 16.72°C to 22.98°C (Fig. 3D), which is 2-2.5°C higher both from lower and upper limits than 1991 of the same season. Out of total area, 75% area is characterized by temperature level ranges from 19.22°C to 21.10°C. Mean and CV of temperature of this phase are respectively 19.97°C and 4.11%. Temperature spread is high both in western and eastern periphery of the main urban land. In the peripheral area rising trend of surface temperature is also identical with core urban area.

In pre monsoon or summer season, 2010 temperature was within the range of 26.83°C to 36.98°C which is 3.20°C higher than 1991. This LST is about 7°C lower than mean air temperature of the same period (Fig. 3E).

Increasing trend of temperature is also reflected in air temperature. Out of the total area, 77% was characterized by a temperature ranged from 28.86°C to 33.93°C. Mean temperature in this period was 31.47°C. and coefficient of variation (CV) was 5.32% which was 0.99% higher than in 1991. The northern part of the main urban area recorded the maximum temperature. This area is characterized by one of the main dense market (Netaji market), busiest traffic node and garlands of hard ware shops.

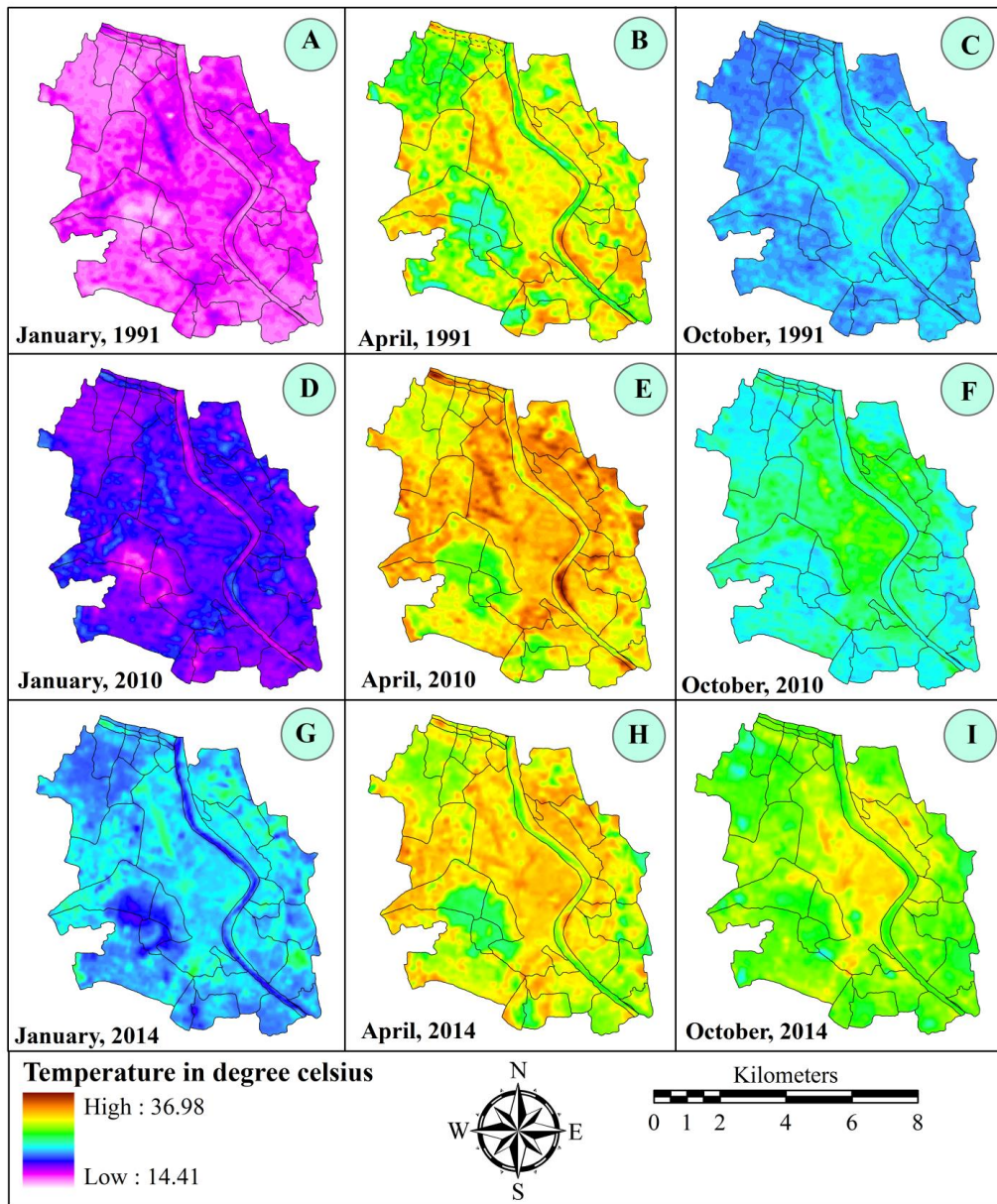


Fig. 3 Land surface temperature A) January 1991 B) April 1991 C) October 1991 D) January 2010 E) April 2010 F) October 2010 (G) January 2014 (H) April 2014 (I) October 2014 based on LANDSAT images

The mean LST was 1.98°C higher than in 1991 in the monsoon season. In 2010, the LST was in range of 22.98°C to 30.58°C (Fig. 3F). Out of total area, 86.08% was characterized by temperatures ranging from 23.73°C to 26.01°C . The mean temperature was 25.37°C and the CV is 4.70% (Table 5).

Seasonal temperature dynamics (winter, pre-monsoon and monsoon) in 2014

In the winter period of 2014, the LST ranged from 20.17°C to 27.30°C and the mean temperature was 23.39°C which was 3.42°C higher compared to 2010 (Fig. 3G). The CV values in this season in all phases establish the fact that there was marginal increase of LST (Table 5).

In the summer season of 2014, the LST varied from 25.22°C to 34.60°C and mean temperature was 30.36°C which was 1.11°C lower than during the previous phase

(Fig. 3H). Actually, 4 days antecedent moisture caused by nor wester lowered surface temperatures. Out of the total area, 87% was characterized by temperatures between 28.03°C to 32.72°C .

In the monsoon of 2014, the LST ranged from 23.63°C to 33.66°C and the mean temperature was 28.70°C which was 3.33°C higher than in 2010 (Fig. 3I). The lowest temperature limit had increased by 0.65°C and the upper temperature limit with 3.08°C compared to the same period in 2010. Out of total area, 87.75% was characterized by temperatures between 26.63°C and 30.65°C .

The present work shows that not only the metropolitan city, but small urban centre like EBM are also gaining temperatures, which is not a good sign for the ambient living conditions. Figure 4 clearly displays the comparative pattern of areal proportion under different

range of temperature since 1991 to 2014 both for summer and winter periods. From this diagram, it can be observed that a larger proportion of the area has shifted to higher temperature classes. For example, only 2.3% area was under the LST above 33°C in 1991 but it is raised to almost 5% in 2014. Such trend is also noticed for other classes also during summer period. Similarly, in winter time, in 1991, no such area was found where LST was 20°C but in 2014 29% area was found where LST is above 23°C.

Table 5 Coefficient variation of temperature in selected time periods

Season	Year	Tmin (°C)	Tmax (°C)	Tmean (°C)	SD	CV (%)
January	1991	14.41	20.34	17.24	0.70	4.04
	2010	16.72	22.98	19.97	0.82	4.11
	2014	20.17	27.30	23.39	1.01	4.33
April	1991	23.99	34.64	29.67	1.94	6.53
	2010	26.83	36.98	31.47	1.67	5.32
	2014	25.22	34.60	30.36	1.64	5.40
October	1991	21.66	28.09	23.40	0.79	3.36
	2010	22.98	30.58	25.37	1.19	4.70
	2014	23.63	33.66	28.70	1.28	4.47

Multicriteria Land Surface Temperature (McLST) models

As mentioned before, the McLST models have been calculated based on six data layers (factors) which control temperature variation. The LST models calculated from the Landsat images and the McLST models have been prepared for the same period of time. Such models will help to understand-whether McLST models can explain LST variation.

Models for 1991

The WLC values varied from 2.17 to 8.87 during winter, 1.61 to 8.69 in summer and 1.95 to 8.57 in monsoon seasons (Fig. 5A, 5B and 5C). In all seasons, higher WLC

values were noticed in the main urban land and some parts of peripheral urban areas where urban extension has already proliferated.

Models for 2010

In 2010, WLC varied from 1.45 to 9.04 in winter, 1.60 to 9.70 in summer and 1.74 to 9.39 in the monsoon or rainy season (Fig. 5D, 5E and 5F). In all seasons, the upper limit of WLC was above 9, while they were below 9 in 1991. This does indicate that LST has raised between 2010 and 2014. The LST trend extracted from multicriteria LST models shows the same pattern as the extracted surface temperature models from Landsat images during the respective seasons. On average surface, the temperature increased with 2.5°C in 2010 compared to 1991.

Models for 2014

In 2014, WLC varies from 1.26 to 9.41 in winter, 2.24 to 9.14 in summer, and 2.54 to 9.35 in rainy season (fig. 5G, 5H, 5I). WLC values at the lower end had raised to some extent indicating rise of LST in the relatively low temperature zones. At the same time, the upper limit of WLC values was also consistently high in all seasons pointing out high LST. From the Landsat based LST models, it was clear that, except in pre-monsoon time, the temperature raised by 3 to 3.5°C in comparison to 2010. Mainly, growing urban intensity could explain this trend.

Spatial Association between LST and McLST models

Spatial correlation analysis is carried out between the models for the respective periods to bring out the fact that these models are spatially associated. In all seasons and selected seasons, correlation coefficient values vary from 0.44 to 0.81 (Table 6) and all values are significant at 99% confidence level. Therefore, these models can be considered as spatially associated. Moreover, the scholarly works carried out by Kawashima et al. (2000) clearly indicates that the mean air temperature is 7° to 9.6°C higher than surface temperature. If same line of thinking could be followed, such association is existing. For further analysis of the relationship, the correlation is also calculated between the two models based on different landuse/landcover classes. In summer period, this correlation coefficient is very high (0.93) in case of built up land, -0.57 in vegetated land, and -0.52 in case of moist land and water bodies. In the core area,

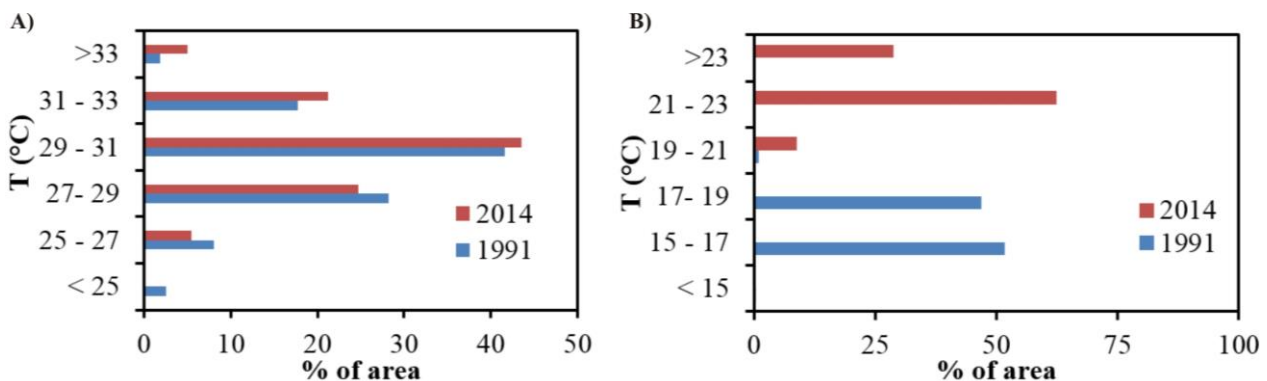


Fig. 4 A) Changing pattern of heat zone (intensity) during April; B) during January in 1991 and 2014

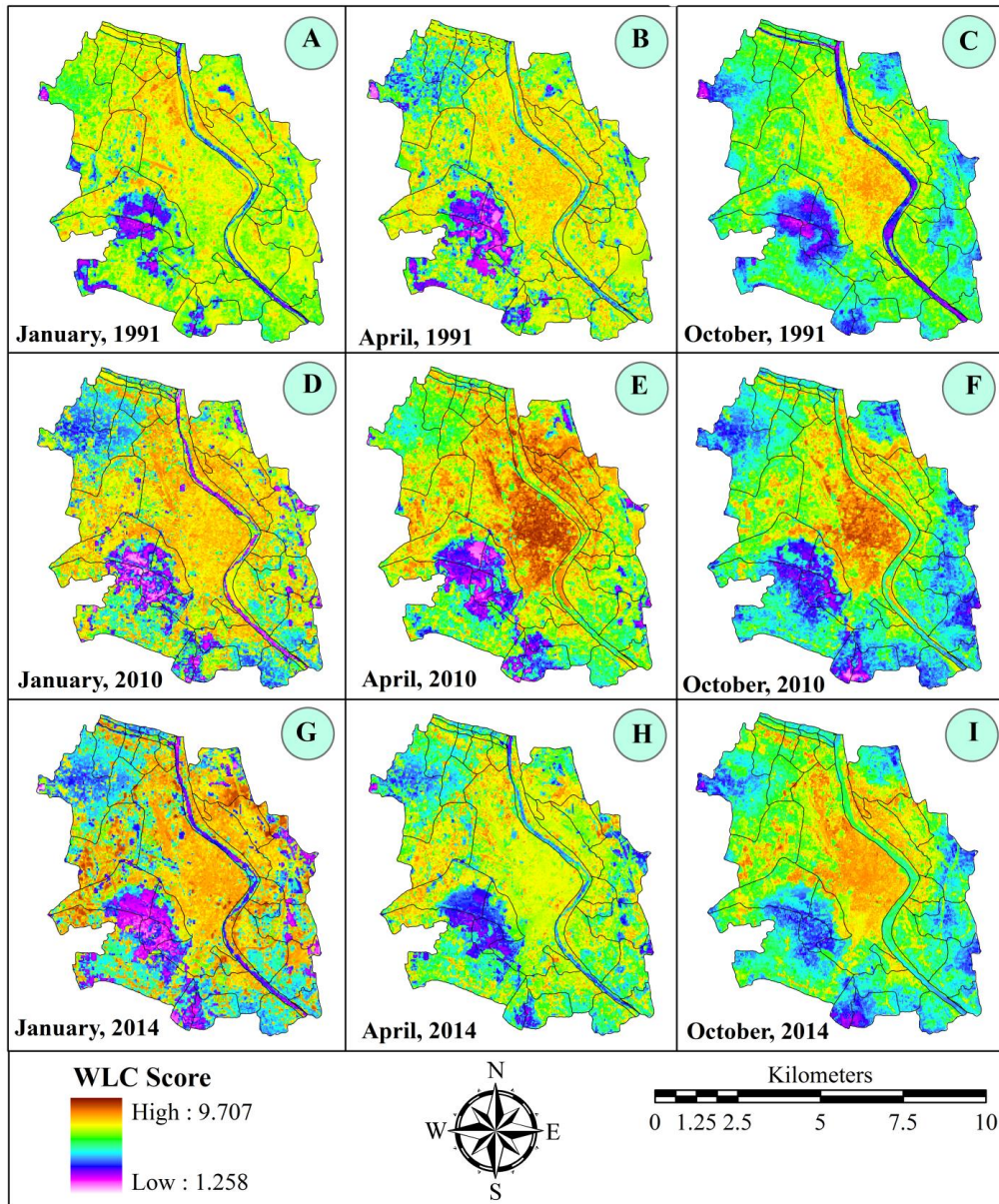


Fig. 5 Multicriteria LST models A) January 1991 B) April 1991 C) October 1991, D) January 2010 E) April 2010 F) October 2010 G) January 2014 H) April 2014 I) October 2014 based on driving factors

this relation is very strong in most of the periods ($r = 0.86-0.93$) while in the peripheral area, the relation is quite weak and varying due to significant differences in landuse/landcover types. In most cases, the strength of the relationship increases over time. Even in the peripheral land, the intensity of temperature rise is mentionable.

Table 6 Degree of correlation between actual and potential temperature models (every correlation coefficient has a significance level of 99%)

Time	Pre-Monsoon	Monsoon	Winter
1991	0.68	0.62	0.51
2010	0.75	0.81	0.60
2014	0.44	0.69	0.68

The McLST models do not directly provide an absolute LST value but the relative temperature differences

can be explored. Relative patterns of WLC values do indicate relative rise or fall of LST. If some random field recording of temperature is made for different sites within the study area and tallying with WLC values, such qualitative McLST models can be quantified.

Factorial analysis

From the selected driving factors of temperature in local scale, it was identified that NDBI most strongly affects the surface temperature followed by land use and major roads. The correlation value between NDBI and LST ranges from 0.42 to 0.80 and mean value for all seasons is 0.66 (Table 7). Densely settled building with very narrow inter buildings spacing, high rise building, expanding roads etc. are some triggering vectors behind the trend of rising temperatures in the urban area. Decreasing canopy cover and increasing concrete impervious surface modifies thermal processes in urban regions, thus causing 2° -

3.5°C higher temperatures compared to rural areas and this effect is known as urban heat island effect (Ogashawara and Bastos, 2012). Dense mango orchard in the north western part of the study area recorded relatively low LST. But the LST condition is not fixed over time, it also increases. This condition results in confusion regarding the role of local driving factor behind temperature changes. Alteration of the hydrologic cycle represents the most significant urban water quality issue at hand today (DeBusk et al., 2010) because storm water runoff from impervious surfaces creates water quality problems including higher water temperatures and elevated levels of contaminants in surface waters (Davis et al., 2010). This effect can immediately influence the nearby Chatra wetland which is considered as kidney of the town (Kar and Pal, 2012). Lack of impoundments within the town accelerates rain water to run down with a fast rate and it also causes rise of LST even in the monsoon season. Low recharge due to high impervious land reduces moisture availability in pore space of the top and sub soil. So, when incident sun rays strike on surface, they penetrate much deeper into the part of the soil strata and enhance surface temperature. The impact of NDVI is prominent during the pre monsoon season but its impact is less obvious during the monsoon because monotonization of surface in regard to high moisture availability. Major roads, specifically the crowded NH34, enhance temperature levels along their axis and their influence is clearly visible in both the Landsat image based LST models and McLST models created for different seasons. Other roads also influence LST in same trend but not with the same intensity. This sort of result is also found in the work of Weng et al. (2004). The modification of LULC associated with urbanization has altered the thermal properties of land, thereby changing the energy budget, creating the UHI as also reported by Xiong et al. (2012) in his work. Brick kiln factories (15 nos.) in the north western part (Bagbari region) of the study area highly increased temperature. Actually this layer is not separately taken into consideration because of its identical emissivity with built up area. The impact of water bodies on lowering temperature is reflected by the models. Chatra wetland (>4 km²), located at south western part of the study area, not only decreases its own temperature but also helps to reduce the temperature of its surroundings. The turbidity level of this wetland has been rising over time and as a result, even in the wetland domain the temperature has also raised up. Related to this, it could

be mentioned that in last 20 years more than 50% of the total wetland area has been converted or will be converted into built up land (Kar and Pal, 2012). Therefore, these areas will also show an increased temperature in the future. The railway station modifies the temperature in an isolated manner, mainly in the station premises. All the discussion imparts to the models prepared from Landsat images and multi criteria approaches and therefore these are comparable.

CONCLUSIONS

It can be said that surface temperature is rising over time in all seasons and the intensification of concrete surfaces within the urban environment and urban expansion in its peripheral zones increases temperature. Both types of LST models point out the unidirectionality of the temperature change. Land use change in terms of installing brick kiln industries, transforming of wetland into urban land, exchange of land between mango orchard and agricultural land etc. are some prime causes for surface temperature change in the urban fringe area. Expansion of concrete surfaces, intensification of built up land, high rise building etc. are some reasons behind increasing temperature in the urban heart land. Considering this trend, immediately land transformation policies should be reviewed specially regarding transforming mango orchard and wetland into built up land. Wetland and forest land can mediate temperature condition in their surroundings.

Urbanization is the main driving process of land cover changes and consequently of change of LST. However, unless undertaking a radical urban decentralization policy, it is difficult to stop or reverse the urbanization process even to the medium and small cities because their function as facility hub.

Vegetation management policies (e.g., green belt) can be implemented that would contain making space for green belts, can consequently help reducing the UHI effect. In addition, policies must not be limited to horizontal growth management only. Additional consideration to implement new urbanism (e.g., green building) concepts in the planning permission (or development assessment) stage of development would also help reducing the LST. English Bazaar Municipality, a small town is so congested in its core part, it is quite difficult make more space available for greening and reducing land surface temperature,

Table 7 Average and range of degree of correlation between LST and selected factors in different seasons

Parameters	Range of winter season	Average of winter season	Range of pre-monsoon	Average of pre-monsoon	Range of monsoon	Average of monsoon
Landuse	0.06-0.59	0.38	0.22-0.41	0.32	0.07-0.07	0.07
NDBI	0.61-0.68	0.65	0.42-0.80	0.67	0.62-0.74	0.66
NDVI	0.07-0.17	0.12	0.25-0.65	0.41	0.23-0.41	0.29
NDWI	0.05-0.37	0.17	0.16-0.48	0.31	0.16-0.27	0.24
Major Road	0.17-0.27	0.22	0.26-0.30	0.27	0.39-0.44	0.42
Railway Station	0.04-0.13	0.07	0.07-0.21	0.11	0.13-0.38	0.27

but further growth should be happening using the new urbanism concepts. Existing roof area can be surfaced with horticulture based plants. At present, municipal rules regarding keeping space between two buildings is only 1 foot but this is too narrow. So, this inter building space policy should be reconsidered. One of the valuable environmental limbs is Chatra wetland located in the south western part of this city that should be intensively preserved. Unfortunately, this wetland is rapidly reclaimed by built up area through urban sprawl. At any cost, it should be protected. Association of such wetland can to some extent decelerate the rise of temperature. Dispersion of urban population through expanding urban structure toward peripheral areas can also reduce temperature. Keeping vacant space with less concrete structures can help to reduce the rising temperature effect. So it is inferred that there is a dire need for continuous monitoring of city's landuse/landcover dynamics and to devise scientific and sustainable urban landuse policies with the purpose to monitor the phenomenon of intensification of UHI.

References

- Alavipannah S., Wegmann, M., Qureshi, S., Weng, Q., Koellner, T. 2015. The Role of Vegetation in Mitigating Urban Land Surface Temperatures: A Case Study of Munich, Germany during the Warm Season, *Sustainability*, 7, 4689–4706; DOI: 10.3390/su7044689.
- Buyantuyev, A., Wu, J. 2010. Urban heat islands and landscape heterogeneity: linking spatiotemporal variations in surface temperatures to land-cover and socioeconomic patterns. *Landscape Ecology* 25: 17–33. DOI: 10.1007/s10980-009-9402-4
- Carver, S. J. 1991. Integrating multi-criteria evaluation with geographical information systems. *International Journal of Geographical Information Systems* 5 (3), 321–339. DOI: 10.1080/02693799108927858
- Central Ground Water Board, Ministry of Water Resources, Government of India 2010. Ground Water Scenario of India 2009-10, 8–10.
- Chen, X.L., Zhao, H. M., Li, P. X., Yin, Z. Y. 2006. Remote sensing image-based analysis of the relationship between urban heat island and land use/cover changes, *Remote Sensing of Environment* 104, 133–146. DOI: 10.1016/j.rse.2005.11.016
- Choudhury, B. J. 1987. Relationships between vegetation indices, radiation absorption and net photosynthesis evaluated by a sensitivity analysis. *Remote Sensing of the Environment* 22, 209–233. DOI: 10.1016/0034-4257(87)90059-9
- Dai, X., Zhongyang, G., Zhang, L., Li, D. 2010. Spatiotemporal exploratory analysis of urban surface temperature field in Shanghai, China. *Stochastic Environmental Research & Risk Assessment* 24, 247–257. DOI: 10.1007/s00477-009-0314-2
- Davis, A. P., Traver, R. G., Hunt, W. F. 2010. Improving urban stormwater quality: Applying fundamental principles. *J. Contemp. Water Res. Educ* 146, 3–10. DOI: 10.1111/j.1936-704x.2010.00387.x
- DeBusk, K., Hunt, W. F., Hatch, U., Sydorovych, O. 2010. Watershed retrofit and management evaluation for urban stormwater management systems in North Carolina. *J. Contemp. Water Res. Educ*, 146, 64–74. DOI: 10.1111/j.1936-704x.2010.00392.x
- Deosthali, V., 2000. Impact of rapid urban growth on heat and moisture islands in Pune City, India. *Atmospheric Environment* 34, 2745–2754. 10.1016/s1352-2310(99)00370-2
- Ding, H., Shi, W. 2013. Land-use/land-cover change and its influence on surface temperature: A case study in Beijing city. *Int. J. Remote Sens.*, 34, 5503–5517. DOI: 10.1080/01431161.2013.792966
- Eastman, J. R. 1997. Idrisi for Windows, Version 2.0: Tutorial Exercises, Graduate School of Geography—Clark University, Worcester, MA.
- Essa, W., Verbeiren, B., van der Kwast, J., van de Voorde, T., Batelaan, O. 2012. Evaluation of the DisTrad thermal sharpening methodology for urban areas. *Int. J. Appl. Earth Obs. Geoinf.* 19, 163–172. DOI: 10.1016/j.jag.2012.05.010
- Gémes, O., Tobak, Z., Leeuwen, B. V. 2016. Satellite based analysis of surface urban heat island intensity, *Journal of environmental geography* 9 (1–2), 23–30. DOI: 10.1515/jengeo-2016-0004
- Giridharan, R., Ganesan, S., Lau, S. S. Y. 2004. Daytime urban heat island effect in high-rise and high-density residential developments in Hong Kong. *Energy and Buildings* 36(6), 525–534. 10.1016/j.enbuild.2003.12.016
- Grover, A., Singh, R. B., 2015. Analysis of Urban Heat Island (UHI) in Relation to Normalized Difference Vegetation Index (NDVI): A Comparative Study of Delhi and Mumbai, *Environments* 2015, 2, 125–138.
- Gulácsi, A., Kovács, F. 2015. Drought Monitoring with Spectral Indices Calculated from Modis Satellite Images in Hungary, *Journal of Environmental Geography* 8 (3–4), 11–20, DOI: 10.1515/jengeo-2015-0008.
- Jalan, S., Sharma, K. 2014. Spatio-Temporal Assessment Of Land Use/Land Cover Dynamics And Urban Heat Island Of Jaipur City Using Satellite Data, The International Archives of the Photogrammetry, Remote Sensing and Spatial Information Sciences, Volume XL-8, 767–772.
- James, M. M., Charles, N. M. 2014. Dynamism of Land use Changes on Surface Temperature in Kenya: A Case Study of Nairobi City, *International Journal of Science and Research* 3 (4), 38–41.
- Kar, S., Pal, S. 2012. Changing Land use Pattern in Chatra Wetland of English Bazar Town: Rationale and Flaws. *International Journal of Humanities and Social Sciences* 2(2), 201–206.
- Kawashima, S., Ishida, T., Minomura, M., Miwa, T. 2000. Relations between Surface Temperature and Air Temperature on a Local Scale during Winter Nights. *Journal of Applied Meteorology* 39, 1570–1779. DOI: 10.1175/1520-0450(2000)039<1570:rbstaa>2.0.co;2
- Keller, C. F. 2008. Global warming: a review of mostly settled issue. *Stochastic Environmental Research & Risk Assessment*, DOI: 10.1007/s00477-008-0253-3.
- Khatun, S., Pal, S. 2016. Identification of Prospective Surface Water Available Zones with Multi Criteria Decision Approach in Kushkaran River Basin of Eastern India, *Archives of Current Research International* 4(4): 1–20, DOI:10.9734/ACRI/2016/27651.
- Kibert, C. J. 2012 *Sustainable Construction: Green Building Design and Delivery*; 3rd ed.; John Wiley and Sons, Inc: Hoboken, NJ, USA, p. 236.
- Kuang, W., Dou, Y., Zhang, C., Chi, W., Liu, A., Liu, Y., Zhang, R., Liu, J. 2015a. Quantifying the heat flux regulation of metropolitan land use/land cover components by coupling remote sensing modeling with in situ measurement. *J. Geophys. Res. Atmos.* 120, 113–130. DOI: 10.1002/2014jd022249
- Kuang, W., Liu, Y., Dou, Y., Chi, W., Chen, G., Gao, C., Yang, T., Liu, J., Zhang, R. 2015b. What are hot and what are not in an urban landscape: Quantifying and explaining the land surface temperature pattern in Beijing, China. *Landsc. Ecol.* 30, 357–373. DOI: 10.1007/s10980-014-0128-6
- Landsat Project Science Office 2002. Landsat 7 Science Data User's Handbook. URL: http://ltpwww.gsfc.nasa.gov/IAS/handbook/handbook_toc.html, Goddard Space Flight Center, NASA, Washington, DC (last date accessed: 10 September 2003).
- Landsberg, H. E. 1981 *The Urban Climate*. New York: Academic Press.
- Li, L., Tan, Y., Ying, S., Yu, Z., Li, Z., Lan, H. 2014. Impact of land cover and population density on land surface temperature: case study in Wuhan, China. *Journal of Applied Remote Sensing* 8, DOI: 1117/1.JRS.8.084993.
- Li, Y. Y., Zhang, H., Kainz, W. 2012. Monitoring patterns of urban heat islands of the fast-growing Shanghai metropolis, China: Using time-series of Landsat TM/ETM+ data. *Int. J. Appl. Earth Obs. Geoinf.* 19, 127–138. DOI: 10.1016/j.jag.2012.05.001
- Liu, L., Zhang, Y. 2011. Urban heat island analysis using the Landsat TM data and ASTER data: A Case study in Hong Kong. *Remote Sens.* 3, 1535–1552. DOI: 10.3390/rs3071535
- Liu, Y., Hiyama, T., Yamaguchi, Y. 2006. Scaling of land surface temperature using satellite data: A case examination on ASTER and MODIS products over a heterogeneous terrain area. *Remote Sensing of Environment*, 105, 115–128. DOI: 10.1016/j.rse.2006.06.012
- Malczewski, J. 2004 GIS-based land-use suitability analysis: a critical overview. *Progr. Plann.* 62 (1), 3–65. DOI: 10.1016/j.progress.2003.09.002
- McFeeters, S. K. 1996. The use of normalized difference water index (NDWI) in the delineation of open water features. *International*

- Journal of Remote Sensing* 17(7), 1425–1432. DOI: 10.1080/01431169608948714
- McMillin, L.M. 1975 Estimation of sea surface temperature from two infrared window measurements with different absorptions. *Journal of Geophysical Research* 80, 5113–5117. DOI: 10.1029/jc080i036p05113
- Monserud, R. A., Leemans, R. 1992. Comparing global vegetation maps with the Kappa statistic, *Ecological Modelling* 62, 275–293. DOI: 10.1016/0304-3800(92)90003-w
- Neteler, M. 2010. Estimating daily land surface temperatures in mountainous environments by reconstructed MODIS LST Data. *Remote Sensing* 2, 333–351. DOI: 10.3390/rs1020333
- Nichol, J. E., Hang, T. P. 2012. Temporal characteristics of thermal satellite images for urban heat stress and heat island mapping, *ISPRS Journal of Photogrammetry and Remote Sensing* 74, 153–162. DOI: 10.1016/j.isprsjprs.2012.09.007
- Nieuwolt, S. 1966. The urban microclimate of Singapore. *The Journal of Tropical Geography* 22, 30–37.
- Ogashawara, I., Bastos, V. S. B. 2012. A quantitative approach for analyzing the relationship between urban heat islands and land cover. *Remote Sens.* 4, 3596–3618. DOI: 10.3390/rs4113596
- Park, H. S. 1986. Features of the heat island in Seoul and its surrounding cities. *Atmos. Environ.* 20, 1859–1866. DOI: 10.1016/0004-6981(86)90326-4
- Peng, S., Piao, S., Ciais, P., Friedlingstein, P., Otle, C., Bréon, F., Nan, H., Zhou, L. 2012. Myneni, R. Surface Urban Heat Island Across 419 Global Big Cities. *Environ. Sci. Technol.* 46, 696–703. DOI: 10.1021/es2030438
- Saaty, T.L. 1980. *The Analytic Hierarchy Process*, New York: McGraw Hill. International. Translated to Russian, Portuguese, and Chinese, Revised editions, Paperback (1996, 2000), Pittsburgh: RWS Publications.
- Schwarz, N., Lautenbach, S., Seppelt, R. 2011. Exploring indicators for quantifying surface urban heat islands of European cities with MODIS land surface temperatures, *Remote Sens. Environ.* 115, 3175–3186. DOI: 10.1016/j.rse.2011.07.003
- Sharma, R., Joshi, P.K. 2013. Monitoring urban landscape dynamics over Delhi (India) using remote sensing (1998–2011) inputs, *J. Indian Soc. Remote Sens.* 41, 641–650. DOI: 10.1007/s12524-012-0248-x
- Singh, R. B., Grover, A., Zhan, J. 2014 Inter-seasonal variations of surface temperature in the urbanized environment of Delhi using Landsat thermal data. *Energies* 7, 1811–1828. DOI: 10.3390/en7031811
- Stathopoulou, M., Cartalis, C. 2009. Downscaling AVHRR land surface temperatures for improved surface Urban Heat Island intensity estimation. *Remote Sensing of Environment* 113, 2592–2605. DOI: 10.1016/j.rse.2009.07.017
- Townshend, J. R., Justice, C. O. 1986 Analysis of the dynamics of African vegetation using the normalized difference vegetation index. *International Journal of Remote Sensing*, 7(11), 1435–1445. DOI: 10.1080/01431168608948946
- UNFPA 2007. *The state of world population 2007: Unleashing the potential of urban growth*. United Nations Population Fund, United Nations Publications.
- Wan, Z., Dozier, J. A. 1996. Generalized split-window algorithm for retrieving land-surface temperature from space. *IEEE Trans Geosci Remote Sens*, 34, 892–905. DOI: 10.1109/36.508406
- Weng, Q. 2001. A remote sensing-GIS evaluation of urban expansion and its impact on surface temperature in the Zhujiang Delta, China. *International Journal of Remote Sensing*, 22, 1999–2014.
- Weng, Q., Lu, D., Schubring, J. 2004 Estimation of land surface temperature-vegetation abundance relationship for urban heat island studies, *Remote Sensing of Environment* 89, 467–483. DOI: 10.1016/j.rse.2003.11.005
- Weng, Q., Yang, S. 2004. Managing the adverse thermal effects of urban development in a densely populated Chinese city. *J. Environ. Manag.* 70, 145–156. DOI: 10.1016/j.jenvman.2003.11.006
- Xiao, R. B., Ouyang, Z. Y., Zheng, H., Li, W. F., Schienke, E. W., Wang, X. K. 2007. Spatial patterns of impervious surfaces and their impact on land surface temperature in Beijing, China. *J. Environ. Sci.* 19, 250–256. DOI: 10.1016/s1001-0742(07)60041-2
- Xiong, Y., Huang, S., Chen, F., Ye, H., Wang, C., Zhu, C. 2012. The impacts of rapid urbanization on the thermal environment: A remote sensing study of Guangzhou, South China. *Remote Sens.* 4, 2033–2056. DOI: 10.3390/rs4072033
- Yuan, F., Bauer, M. E. 2007. Comparison of impervious surface area and normalized difference vegetation index as indicators of surface heat island effects in Landsat imagery. *Remote Sensing of Environment* 106, 375–386. DOI: 10.1016/j.rse.2006.09.003
- Zha, Y., Gao, J., Ni, S. 2003. Use of normalized difference built-up index in automatically mapping urban areas from TM imagery. *International Journal of Remote Sensing* 24(3), 583–594. DOI: 10.1080/01431160304987
- Zhang, H., Qi, Z. F., Ye, X.Y., Cai, Y. B., Ma, W. C. 2013. Analysis of land use/land cover change, population shift, and their effects on spatiotemporal patterns of urban heat islands in metropolitan Shanghai, China. *Appl. Geogr.* 44, 121–133. DOI: 10.1016/j.apgeog.2013.07.021